05

Relaxation of magnetic properties of [Pt/Co]/IrMn multilayer films during annealing and natural aging

© A.N. Orlova,[1] S.A. Gusev,[1] M.V. Sapozhnikov,[1,2] I.Yu. Pashenkin,[1] D.A. Tatarskiy[1,2]

[1] Institute of Physics of Microstructures, Russian Academy of Sciences,
607680 Nizhny Novgorod, Russia
[2] Lobachevsky State University,
603950 Nizhny Novgorod, Russia
e-mail: orlova.anastasia@ipmras.ru

Received April 15, 2024
Revised April 15, 2024
Accepted April 15, 2024

The purpose of the work is to study multilayer Pt/$[Pt/Co]_5$/IrMn films, in which the cobalt thickness varies from 0.6 to 1.5 nm, namely, to study changes in their magnetic properties that occur under the influence of thermal annealing and during natural aging. The samples were prepared by high-vacuum magnetron sputtering; their structure and properties were studied by magneto-optical Kerr magnetometry and transmission electron microscopy. It was found that natural aging only leads to a decrease in the exchange shift, while during thermal annealing in a zero magnetic field, a decrease in the exchange shift is accompanied by an increase in coercivity. These effects are more pronounced in structures with thin films of cobalt, with a thickness of less than 1 nm.

Keywords: ferromagnet, antiferromagnet, exchange bias, coercive force, perpendicular magnetic anisotropy, high-vacuum thermal annealing, tunnel magnetic contacts.

DOI: 10.61011/TP.2024.07.58797.121-24

Introduction

Thin magnetic films with perpendicular magnetic anisotropy (PMA) are currently an integral component of modern magnetoresistive random access memory (MRAM). MRAM element is a tunnel magnetic contact (TMC) consisting of two ferromagnetic layers separated by a tunnel dielectric interlayer. One of the ferromagnetic layers has high magnetic anisotropy and is referred to as the fixed or reference layer, and the second layer may be switched in relatively low fields and is referred to as a free layer. resistance of such contact depends on the mutual orientation of ferromagnetic magnetization. TMC-based perpendicular-anisotropy MRAM has a set of advantages over the „easy-plane“ anisotropy, among which much better scalability, high thermal stability and relatively low density of resistive state switching current may be distinguished. TMC with PMA is used to employ spin-orbital effects for state switching such as the Hall spin effect and VCMA (voltage control of magnetic anisotropy) [1] and to achieve ultra-low switching energies [2].

One of the ferromagnetic layers is a key process element of TMC, a so-called reference or fixed ferromagnetic layer [3]. This layer is also called so because it has fixed magnetic orientation and is not changed when the tunnel magnetic contact is operated. There are two fundamental approaches to form the TMC reference layer. In one case, magnetization orientation of the fixed layer is fixed using antiferromagnetic RKKI (Rudermann–Kittel–Kasuya–Iosida exchange interaction) interlayer exchange interaction with additional ferromagnetic layer through a thin non-magnetic metal interlayer (e.g. rhutenium). Such pair of antiferromagnetically-coupled layers forms a synthetic antiferromagnetic layer [4,5]. In another case, a ferromagnetic layer, e.g. IrMn, is sputtered on the ferromagnetic layer with PMA when the structure id formed. If the ferromagnetic film remains uniformly magnetized during subsequent antiferromagnetic film growth, then the hysteresis loop is displaced at the exchange bias value due to the presence of exchange interaction at the ferromagnetic–antiferromagnetic interface. To induce unidirectional anisotropy, a magnetic-field cooling procedure is used very often when the structure is preliminary heated to the antiferromagnetic locking temperature, i.e. to the temperature below which magnetization relaxation flows less visibly with time. Typical ferromagnetic materials that are used or such structures are Co, CoFe and CoFeB, where PMA is formed on interfaces with thin Pt layers, and IrMn, FeMn, NiMn, PtMn, PtPdMn are used as antiferromagnetic materials [6–12].

PMA structures where exchange shift of the magnetization curve is implemented may serve as a medium where skyrmion lattices are formed in a zero external magnetic field which may be useful for the development of magnetoresistive memory based on skyrmion motion. inhomogeneous magnetic states, i.e. skyrmion states, were detected in our grown structures examined using the transmission electron microscope in the Lorentz mode. Skyrmions were observed in films with thick cobalt layers (from 1 to 1.5 nm).

Long-term functioning of TMC with process buffer layers is an individual task. It has been found that Mn atom

diffusion at high temperatures (higher than 200°C) results in significant degradation of TMC [13]. The degradation is attributed to restructuring, i.e. Mn atom diffusion through the ferromagnetic–antiferromagnetic interface into the ferromagnetic film during vacuum thermal annealing at temperatures higher than 250–300°C [14,15]. It has been shown before that the thermal resistance (up to 350°C) can be increased using particular antiferromagnetic materials (NiMn, PtMn) [12]. Alternative way to suppress Mn atom diffusion is specific design of ferromagnetic–antiferromagnetic interface: either an amorphous CoFeB layer or closely-packed CoFe layers with body-centered cubic lattice and axial structure (110) [16]. Such structuring suppresses the „low-temperature“ diffusion of Mn atoms associated with the presence of impurity oxygen atoms, while the „high-temperature“ diffusion is associated with vacancies in amorphous CoFeB and grain boundaries in CoFe, but such diffusion cannot be suppressed.

For successful implementation of the tunnel magnetic contact, low-coercive state (avoid broadening of the hysteresis loop in long-term utilization and in periodic heating of TMC) and structure stability (retaining such magnetic properties as exchange bias) shall be implemented simultaneously. The study investigated systematically the hysteresis loop and exchange bias variations in Pt/$[Pt/Co]_5$/IrMn type structures with natural ageing and thermal annealing depending on the Co layer thickness. Long-term exchange shift maintenance mechanisms and possible stabilization of the long-term period by means of properly selected materials system for development of spintronics devices are discussed.

1. Description of samples and experiment procedure

Multilayer nanostructures were made by high-vacuum magnetron sputtering on a Si substrate in a perpendicular magnetic field (50 mT) at room temperature using the ATS-2200 (AJA International Inc.) system. Residual pressure in a growing vessel was not higher than $3 \cdot 10^{-7}$ Torr. Thin-film periodic structures were sputtered from alloyed targets by means of consecutive sputtering of cobalt, platinum, tantalum and 20% iridium and 80% manganese alloy targets. Material deposition rates were as follows: Co — 0.10 nm/s, Pt — 0.22 nm/s, IrMn — 0.033 nm/s, Ta — 0.12 nm/s. Multilayer structures were grown on Si (100) substrate treated in high-frequency argon plasma with an ion energy of ~ 30 eV before the growing process. After sputtering, the samples were subjected to „field cooling“: first, the sample was heated up to 250°C, then placed into 400 mT perpendicular magnetic field, heating was turned off and the sample was cooled in the magnetic field. Ta, Co, Pt were sputtered at room temperature and operating pressure of argon in the growing vessel of 2 mTorr. Operating pressure during IrMn layer growth was 4 mTorr. To ensure homogeneity of layers in the fabricated structures, sputtering was performed onto substrates rotating at 20 rpm.

To produce multilayer structures, 4 nm buffer tantalum and platinum layers were first sputtered onto the Si substrate. Then the periodic Pt/Co structure is grown where 0.6 to 1.5 nm cobalt layers and 1 nm platinum layers are alternated. Then a 5 nm antiferromagnetic IrMn layer is sputtered on the top cobalt layer.. An antiferromagnetic layer is required to fix the magnetization orientation in the ferromagnetic layer due to exchange shift. At the end of sputtering procedure, the whole structure was coated with a 3 nm buffer tantalum layer.

To ensure that the desired structure was achieved, the samples were examined using the LIBRA 200MC (Carl Zeiss, Jena) transmission electron microscope. For electron microscope investigations, cross-sectional cuts of the grown films were made by means of special preparation. The sample preparation procedure was arranged as follows. Initially, 4×5 mm rectangular plates are cut from the samples. Then a sample „package“ is made from them using two-component epoxy resin with the structure placed in the center between the sacrificial layers. Then, a cylinder containing the area of interest is drilled out of the package and glued into a 3 mm brass tube. Then, the workpiece is sawn into $\sim 0,5$ mm discs using an ultrathin diamond disc. The subsequent polishing of the thin disc is conducted in two stages: the first stage is mechanical manual treatment using sand paper with successive grain size reduction to $\sim 100\,\mu$m, the second stage is automated sample thinning performed using a grinding machine (dimpler) making a dimple from 40 to 60 μm in depth in the disc. Precision ion-beam etching by argon atoms using the Fischione TEM Mill system performed until perforation is made in the center of the dimple was the final stage of sample preparation. A cross-section image of one of the structures made using the high-resolution transmission electron microscopy (HRTEM) is shown in Figure 1.

The cross-section image clearly shows that the Co and Pt layers are not mixed and structural periodicity of the

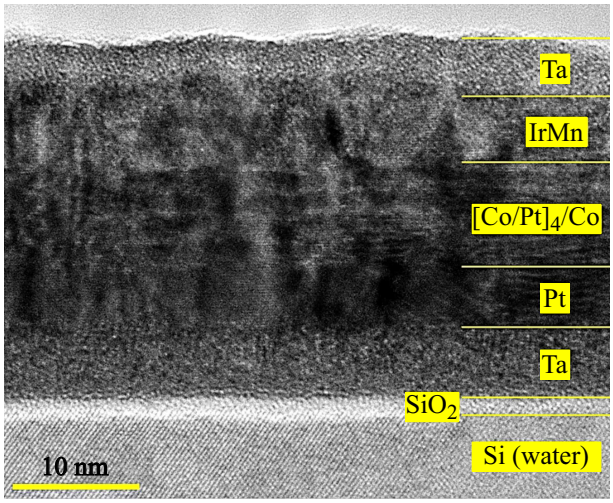

Figure 1. HRTEM image of the multilayer periodic Ta(5)/Pt(4)/[Pt(1)/Co(0.6)]$_5$/IrMn(5)/Ta(3) structure. Numbers in brackets are the layer thickness in nanometers.

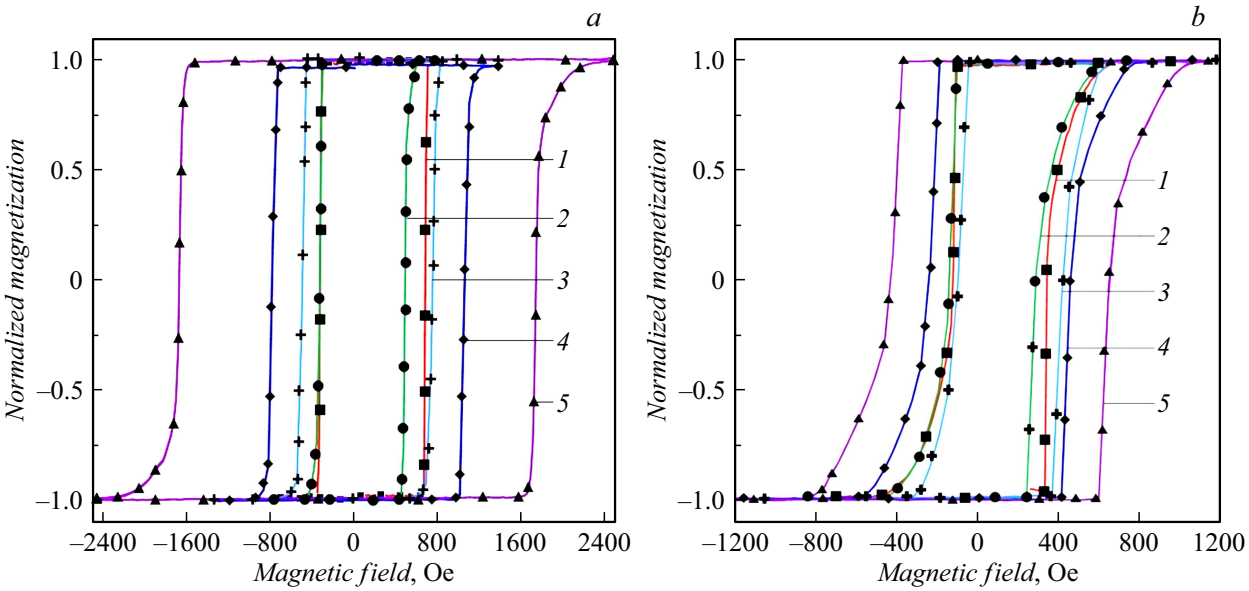

Figure 2. Magnetization curves of the test structures: *a* — sample with 0.6 nm Co layers; *b* — sample with 1.1 nm Co layers. Curve *1* — initial state of structures; curve *2* — structure state almost a year later; curve *3* — reduced state immediately after magnetic-field annealing; curves *4* and *5* — states after thermal annealing with different times without external magnetic field (1 h and 3 h, respectively).

multilayer Co/Pt film is maintained. Also note that the thicknesses of the grown layers correspond to the initially specified values.

Magnetic properties of the films were controlled and hysteresis loops were measured using a magnetometric system by measuring the polar-geometry Kerr effect by crossed polarizers at room temperature. Highly stabilized 632 nm He−Ne-laser (Thorlabs HRS015B) was used as a radiation source. Laser generates *p*-polarized monochromatic radiation focused on the surface of the sample placed in a special holder between electromagnet poles with a field up to 0.5 T. Power of the reflected radiation transmitted through the analyzing polarizer was measured using Si photodiode. Magnetization hysteresis loops were measured as the dependence of the reflected light polarization rotation angle on the applied magnetic field.

The study program was arranged as follows. Magnetization loops were measured immediately after fabrication. The first part of the experiment included the study of magnetic properties variation during temporal ageing. During the year, the samples were stored in closed cups in atmosphere at room temperature. Conditions were provided to keep the samples away from sun and artificial light, therefore the samples were stored in a dark place. Then, magnetooptical investigation was performed again to estimate the variation of magnetic properties with time. Using the recorded magnetization curves, we suggested that the structures show different changes during storage depending on the ferromagnetic layer thickness. After completion of the temporal ageing study, the samples were annealed to 250°C in a 400 mT perpendicular magnetic field. It was found that such annealing resulted in reduction of properties of a group of samples. After each sample handling, magnetooptical measurements were performed to record the changes.

The second part of the experiment includes a study for verification of the temperature effect on the exchange shit and film coercivity. Therefore, the further reduced structures were subjected to high-vacuum thermal annealing without magnetic field. It was assumed that film heating would accelerate natural ageing of structures and cause the same changes as were observed during temporal ageing, i.e. exchange bias disappearance. However, after thermal annealing without magnetic field, magnetic properties of the samples were changed in a different way and our initial assumption was not confirmed or all samples from the series of interest because the structures showed different stability to temperature manipulations.

Thus, the study involved 5 key measurements that were marked on the curves in Figure 2. Measurement № 1 was performed in April 2023 and recorded the initial state of the sample immediately after sputtering. Initial films demonstrate the „easy-axis“ perpendicular magnetic anisotropy. Then the samples were removed into the corresponding storage conditions to hold the time interval, and further measurements were performed at the end of February 2024. Measurement № 2 was performed without additional actions to estimate the change in structure states with time. Right after that, the samples underwent thermal annealing in magnetic field to restore the hysteresis loops, and then measurement № 3 was performed. Then the samples were annealed at the same temperature, but without magnetic field, to check exactly the thermal effect on the structures. Measurement № 4 was performed after thermal annealing without magnetic field during 1 h. After removal of the hysteresis loops from the structures annealed

Table 1. Main characteristics of the magnetic hysteresis loops for samples with various Co layer thicknesses

Structure	Parameters, Oe	Measurement				
		№ 1(■)	№ 2(●)	№ 3(+)	№ 4(♦)	№ 5(▲)
Co(0.6 nm)	H_c	1140	835	1245	1850	3410
	H_{bias}	130	83	123	125	25
Co(0.9 nm)	H_c	630	625	780	960	1350
	H_{bias}	115	8	110	120	125
Co(1.1 nm)	H_c	465	430	515	700	1080
	H_{bias}	108	75	158	105	110
Co(1.5 nm)	H_c	335	300	405	435	715
	H_{bias}	168	150	158	148	157

Note. H_c — loop width, and H_{bias} — exchange bias, symbols in brackets correspond to the symbols in Figure 2.

during 1 h, it was found that the exchange bias almost disappeared, but still existed in the range up to 150 Oe. Therefore, a hypothesis was proposed that the exchange shift can completely disappear during longer annealing, as a result measurement № 5 was performed — measurement after thermal annealing during 3 h also without external magnetic field. After that, for each magnetization curve, exchange shift and coercivity fields were calculated and, thus, we obtained curves of parameter variation after various manipulations. The curves will be shown below in the experimental findings.

2. Experimental findings and discussion

Temporal ageing was measured for a series of sample with Co thicknesses from 0.6 to 1.5 nm at 0.1 nm interval across the thickness. The test samples may be nominally divided by the magnetization curve shapes into two groups: with thin Co layers (0.6−0.9 nm) and thick Co layers (1.1−1.5 nm). For each of the distinguished groups of samples, a typical form of magnetization loops was obtained, therefore curves for two structures will be provided herein. Each of these structures is a representative of a particular type. The typical forms of sample magnetization curves are shown in Figure 2.

The form of magnetization loops measured by the magnetooptical magnetometry method and shown in Figure 2 is typical for the structures having the „easy-axis“ perpendicular magnetic anisotropy with residual magnetization equal to saturation magnetization. The qualitative form of loops shown in Figure 2 has differences associated with different thickness of ferromagnetic film. Structures with thin Co layers, the magnetization curve is rectangular suggesting that remagnetization occurs immediately from one uniformly saturated state into another uniformly saturated state. On the contrary, for structures with thick Co layers, domains are formed as the magnetic field increases, therefore, complete remagnetization is not observed immediately. The system is switched to the oppositely saturated state only with further increase in the external magnetic field. This results in the magnetization loop with typical „tails“.

The measured structure magnetization curves may be characterized by two main parameters — exchange bias and coercivity. Coercivity in this case means the loop width, and the exchange bias is defined by the position of the loop center on the applied field scale. These loop parameters obtained by measuring the series of samples are shown in Table 1.

The calculations suggest that several magnetic properties variation patterns may be distinguished. Since the parameters of interest are the width and exchange shift of hysteresis loops, the variation trends of these parameters during natural ageing and after thermal impact are shown separately in Table 2.

For clarity, the measurements were presented in graphic form as shown in Figure 3: Figure 3, *a* shows the dependence of hysteresis loop width variation after annealing and a long period of time, and Figure 3, *b* shows the exchange bias variation in structures before and after thermal treatment.

The curve in figure 3 show that the samples with thin and thick Co layers have different changes. However, there is still a common trend — hysteresis loop broadening under thermal annealing. This is because an increase in the mean size of nanocrystallites in films is observed during thermal treatment [17], after which film restructuring takes place. The exchange bias almost disappears in samples with thin Co layers after thermal annealing in the absence of the external magnetic field and during natural ageing. But the exchange bias in structures with thick Co layers (1.0−1.5 nm) is also retained during natural ageing of samples and annealing of the structure, unlike the samples with thin ferromagnetic layers (0.6−0.9 nm), where the exchange bias decreases with time and under a thermal effect. This probably occurs due to pinning between the antiferromagnetic layer and reference ferromagnetic layer,

Table 2. Typical trends and changes in the magnetic properties of films taking place during natural ageing and after thermal annealing

Structure	Natural ageing		Annealing at $H = 0$	
	Width	bias	Width	bias
Thin Co layers (0.6–0.9 nm)	Decreases ↓↓↓	Decreases ↓↓↓	Increases ↑↑↑	Decreases ↓↓↓
Thin Co layers (1–1.5 nm)	Unchanged –	Unchanged –	Increases ↑↑↑	Unchanged –

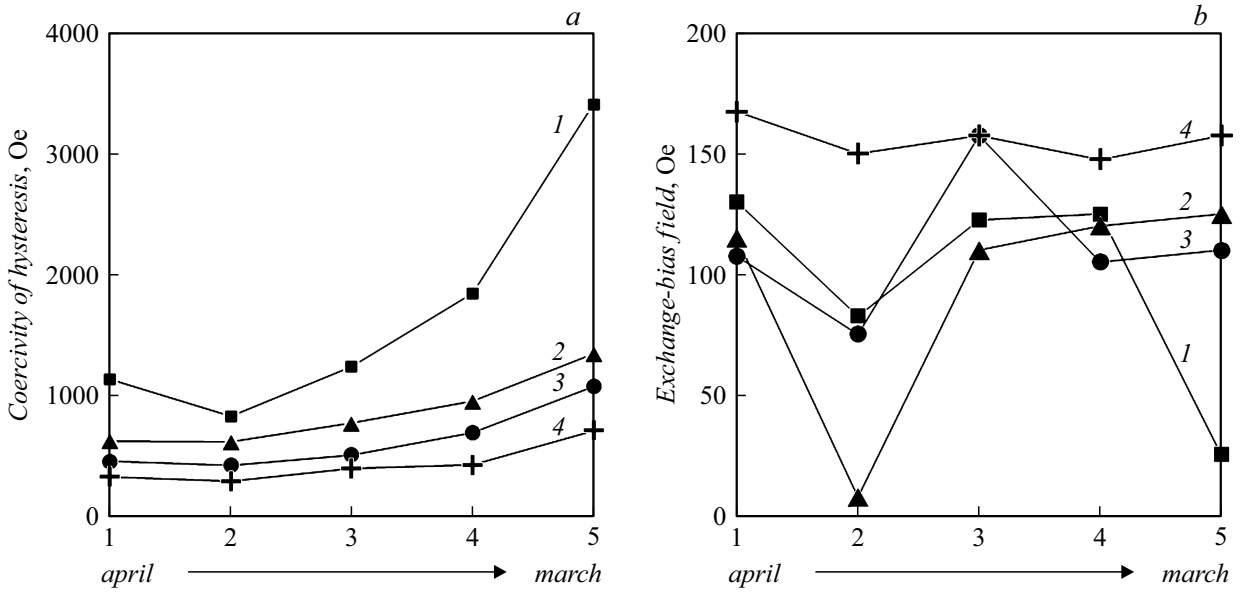

Figure 3. Variation of magnetic properties of structures depending on time: *a* — hysteresis coercivity variation; *b* — exchange bias variation with time and after thermal treatment. Each curve was built depending on the ferromagnetic thickness in the structure: curve *1* with Co thickness 0.6, *2* — 0.9, *3* — 1.1, *4* — 1.5 nm.

and, therefore, the thickness ratio of these layers affected the exchange bias behavior in films.

As mentioned above, different crystallite sizes may affect the magnetic properties of a structure. In this case, this is increase in the nanocrystallite size due to thermal annealing [17]. Analysis of crystallite sizes in films was performed using TEM (Carl Zeiss Libra 200MC). For this, the structures were sputtered onto amorphous silicon nitride membranes with a 50–100 nm electron-transparent window. Crystallite size was estimated using the dark-field image technique. The mean size of coherent scattering areas is determined by means of autocorrelation analysis in polar coordinates that is used to estimate the shape of structure crystallites. Nanocrystallite size before annealing is 3.4 ± 0.4 nm, after annealing the crystallite size is approximately twice as large. The typical form of the dark-field microphotograph of one of the structures made using TEM is shown in Figure 4.

The detail in the right corner in Figure 4 shows the microdiffraction pattern from the selected test area that is represented by a series of concentric circles. The presence of diffraction rings implies polycrystallinity of films with various crystallite orientations.

Thus, the magnetooptical measurements suggest that the exchange bias in structures with thick Co layers is not changed with time and during high-vacuum thermal annealing. The shift field in such samples is resistant to restructuring. In samples with thin ferromagnetic layers, the exchange bias decreases gradually during natural ageing and almost completely disappears under the thermal effect. The same increase in coercivity after thermal treatment was detected in all samples, but the loop width remain unchanged with time.

Currently there is no any reliable explanation of the reasons behind the observed behavior, nevertheless we can propose the following hypothetical explanation of our experimental data. Changes that occur during annealing are probably associated with crystal restructuring and therefore do not depend on the ferromagnetic and antiferromagnetic layer thicknesses. Growth of crystallites results in coercivity

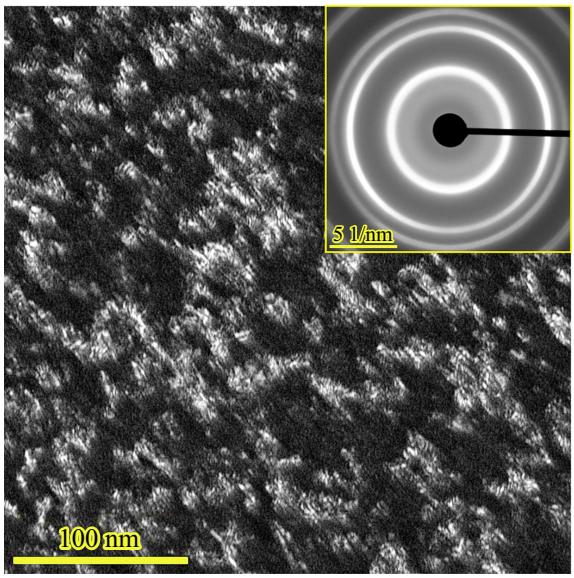

Figure 4. Dark-field photograph of Pt(1)/[Pt(1)/Co(1)]$_5$/IrMn(5) structure and diffraction pattern of the selected area. Numbers in brackets are the layer thickness in nanometers.

increase. Changes caused by temporal ageing are of different nature and occur due to magnetic state relaxation in the antiferromagnetic layer and may be explained by the magnetic resgructuring.

In our samples, the antiferromagnetic layer was applied to the ferromagnetic films and , therefore, the Co layer oriented by the magnetic field of the sputtering system defines the unidirectional magnetic anisotropy orientation, and the Ir−Mn layer is magnetically ordered depending on the Co magnetization orientation. Note that the film interface has subnanometer roughnesses which may result in separation of the antiferromagnetic film into domains. If the exchange-coupled ferromagnetic layer is thin, it cannot prevent gradual domain restructuring in the antiferromagnetic layer resulting in the exchange bias reduction. This process is observed both during temporal ageing and annealing.

Conclusion

The exchange bias tends to decrease with time in structures having the lowest ferromagnetic thickness. But the exchange bias is retained when the ferromagnetic and antiferromagnetic thicknesses become comparable or when the ferromagnetic content becomes higher in the film. Also, broadening of the hysteresis loop is observed in all samples after annealing without magnetic field due to the thermal restructuring.

The obtained data shall be used for the development of tunnel magnetic contacts on the basis of this system of materials with Co layers as reference layers. This is associated with the fact that periodic heating of components might occur in the magnetic memory devices during remagnetization due to the flowing currents. Despite the structures with thick Co layers have narrower hysteresis loops, which is worse in terms of application as the fixed layer, they are more resistant to thermal treatment and temporal degradation, and better retain their initial magnetic properties.

Funding

The study was supported by grant of the Russian Science Foundation № 21-72-10176. Equipment provided by the Common Use Center „Physics and Technology of Micro- and Nanostructures“ (Institute of Physics of Microstructures, Russian Academy of Sciences) was used for the study.

Conflict of interest

The authors declare that they have no conflict of interest.

References

[1] P. Kh. Amiri, K.L. Wang. World Scientif., **02** (03), 1240002 (2012).
[2] P. Salev, I. Volvach, D. Sasaki, P. Lapa, Y. Takamura, V. Lomakin, I.K. Schuller. J. Phys. Rev. B, **107**, 054415 (2023).
[3] M. Wang, Y. Zhang, X. Zhao, W. Zhao. Micromachines, **6** (8), 1023 (2015).
[4] W. Zhao, X. Zhao, B. Zhang, K. Cao, L. Wang, W. Kang, Q. Shi, M. Wang, Y. Zhang, Y. Wang, Sh. Peng, J.-O. Klein, L.A. De Barros Naviner, D. Ravelosona. Materials, **9** (1), 41 (2016).
[5] S.-E. Lee, T.-H. Shim, J.-G. Park. NPG Asia Materials, **8**, 324 (2016).
[6] E.V. Khomenko, N.G. Chechenin, A.Yu. Goikhman, A.V. Zenkevich. Condens. Matter., **88**, 602 (2008).
[7] H. Gao, Y. Liu. AIP Advances, **9**, 015132 (2019).
[8] J. Sort, V. Baltz, F. Garcia, B. Rodmacq, B. Dieny. Phys. Rev. B, **71**, 054411, 2005.
[9] Y.F. Liu, J.W. Cai, S.L. He. J. Phys. D: Appl. Phys., **42** (11), (2009).
[10] Q. Ying, L. Yifan. AIP Advances, **8**, 025314 (2018).
[11] D.S. Shapiro, A.D. Mirlin, A. Shnirman. Phys. Rev. B, **107**, 125404 (2023).
[12] G.W. Anderson, Y. Huai, M. Pakala. J. Appl. Phys., **87**, 5726 (2000).
[13] J.P. Nozieres, S. Jaren, Y.B. Zhang, A. Zeltser, K. Pentek, V.S. Speriosu. J. Appl. Phys., **87**, 3920 (2000).
[14] A. Maesaka, N. Sugawara, A. Okabe, M. Itabashi. J. Appl. Phys., **83**, 7628 (1998).
[15] M. Takiguchi, S. Ishii, E. Makino, A. Okabe. J. Appl. Phys., **87**, 2469 (2000).
[16] Y. Wang, Z.M. Zeng, X.F. Han, X.G. Zhang, X.C. Sun, Z. Zhang. Phys. Rev. B, **75**, 214424 (2007).
[17] S.A. Gusev, D.A. Tatarsky, A.Yu. Klimov, V.V. Rogov, E.V. Skorokhodov, M.V. Sapozhnikov, B.A. Gribkov, I.M. Nefedov, A.A. Fraerman. FTT **55**, 3 (435 2013) (in Russian).

Translated by E.Ilinskaya